Indian Journal of Ecology (2023) 50(3): 802-810
DOI: https://doi.org/10.55362/IJE/2023/3973

Manuscript Number: 3973
NAAS Rating: 5.79

Monitoring Vegetation Health, Water Stress, and Temperature Variation through Various Indices using Landsat 8 Data

Arvind Dhaloiya[1,2], Derrick Mario Denis[1], Darshana Duhan[4], Ritesh Kumar[5], Mahesh Chand Singh[2] and Anurag Malik[3]

[1,2]Department of Irrigation and Drainage Engineering, VIAET, Sam Higginbottom University of Agriculture, Technology and Sciences, Prayagraj-211 007, India
[2]Department of Soil and Water Engineering, Punjab Agricultural University, Ludhiana-141 004, India
[3]Punjab Agricultural University, Regional Research Station, Bathinda-151 001, India
[4]Chaudhary Charan Singh Haryana Agricultural University, Hisar-125 004, India
[5]Haryana Space Applications Centre, Hisar-125 004, India
E-mail: arvinddhaloiya@gmail.com

Abstract: Remote Sensing (RS) may serve as an efficient tool to monitor and assess the water stress, vegetation health, and temperature variations in a region with both time and space. The present study was undertaken to monitor vegetation health, water stress, and temperature variation by estimating nine widely used spectral indices for seven stations (Ambala, Bhiwani, Gurugram, Hisar, Karnal, Narnaul, and Rohtak) located in Haryana State, India using the 30-m Landsat-8 data. The spectral indices were cross-verified with ground observation data collected from the seven stations. The used indices included the Normalized Difference Vegetation Index (NDVI), Soil-Adjusted Vegetation Index (SAVI), Modified Soil-Adjusted Vegetation Index (MSAVI), Normalized Difference Built-up Index (NDBI), Normalized Difference Water Index (NDWI), Normalized Difference Moisture Index (NDMI), Normalized Difference Infrared Index for Band 7 (NDIIB7), and Surface Albedo and Land Surface Temperature (LST). The observed data for all the nine indices for different locations showed large variations throughout the study period (2013–2018). Large variations of LST values were observed during the study period in the study regions. The findings of the study exhibited the ability of RS technology in assessing and monitoring vegetation health, water stress, and temperature variations in the study area. Such a study would be helpful in long-term crop planning in a region concerning the improved monitoring and management of temperature variation and crop water stress.

Keywords: RS, GIS, LST, NDBI, MSAVI, NDWI, NDIIB7

The study of regional eco-environment should focus on economic development and ecosystem conservation (Surya et al 2020). The main reason for the accumulation and expansion of ecological vulnerability is due to the higher rate of human-socioeconomic activity and climate change (Saha et al 2021, Xu et al 2021, Boori et al 2022). RS has emerged as an important tool to measure and track the characteristics of terrestrial ecosystems at several scales due to consistent, extensive coverage and high spatial and temporal resolutions (Gu and Wylie 2015). Data of spatial, spectral and temporal resolutions are acquired for physical processes that take place on Earth using RS techniques such as Landsat Sensors, Multispectral Scanner (MSS), Thematic Mapper (TM), different satellite sensors, and aircraft cameras. In recent years, many coarse and high-resolution RS images are available free of cost to the user and are not limited to commercially available images of very high spatial resolution such as Sentinel and Landsat images. Further, such images are usually acquired with several desired spectral bands, i.e., the near-infrared and thermal bands, thus proving their applicability in natural process modeling such as vegetation health and stress. Land surface reflectance and temperature data can be used to quantify crop water stress using different vegetation and temperature indices calculated from the near-infrared, red, and thermal band (Neale et al 1990, Bausch 1993, Bausch et al 2011, DeJonge et al 2015, Dejonge et al 2016). The vegetation indices were used to estimate fractional vegetation cover add spacing (Trout et al 2008, Johnson and Trout 2012, Kumar et al 2019, Arvind et al 2020, Kumar et al 2021). During the last decades, various studies have been carried out for the assessment of eco-environmental quality. Several techniques like analytical hierarchical process (AHP), the index evaluation method, fuzzy comprehensive evaluation method, matter element analysis, and principal components analysis are used to reveal the regional eco-environmental situation (Zhang et al 2011). The vegetation indices i.e., SAVI, NDVI, MSAVI, etc. have been developed and used in the last half-century. The algebraic combination of spectral bands is the fundamental hypothesis behind the development of these indices, which

can reveal useful biophysical characteristics such as vegetation or leaf structure, coverage, density, spread, water content, and mineral deficiencies (Holben 1986). In addition, factors influencing spectral reflectance's such as soil properties, atmospheric conditions, sensor viewing geometry, and solar illumination should be less susceptible to healthy vegetation indices (Tucker and Garratt 1977, Holben 1986). The leaf structure influences vegetation interactions with sunlight for photosynthesis. The leaves have two procedures, i.e., absorption and scattering of sunlight. At particular wavelengths, plant pigments and water present in the leaves absorb light. Scattering is caused by the leaves' inner composition, whereas the leaf's interior is a labyrinth of air spaces and irregularly water-filled cells. Green leaves absorb most in the blue and red regions and less in the green region (Holben 1986). There is no absorption from upper vision limit of 700 nm to more than 1300 nm. No absorption indicates high rates of reflectance of green vegetation beyond the red band (Tucker and Garratt 1977).

The normalized difference vegetation index (NDVI) value varies from ±1. The dense vegetation here is described by +1; water typically has an NDVI value less than zero (Taloor et al 2021). Here, −1 means the existence of large water bodies (Holben 1986). Specified some typical NDVI values for different types of land use/land cover, where the water value is −0.257. Dwivedi and Sreenivas (2002) considered the limit value of 0.13 of NDVI for the separation of vegetation areas from waterlogged areas using Landsat and IRS-1A (Indigenous state-of-art operating remote sensing satellites) and LISS-I (Linear Imaging Self Scanning Sensor) data. The NDWI was designed to obtain the difference in the signature for water availability in plants (McFeeters 1996, Xu 2006). The NDBI is used to obtain built-up features and ranges between −1 and +1 (Zha et al 2003). The drought index NDIIB7 is used for measuring water stress in vegetation. The interpretation of the NDMI's absolute value makes it possible to identify the farm or field areas with water stress problems instantly. NDMI can be easily interpreted using its value ranges from −1 to +1 (Taloor et al 2021). The NDMI and NDWI are satellite-derived indices to monitor soil and vegetation moisture conditions. In areas with sparse vegetation, the ability of greenness indices for evaluating vegetation is limited due to neighboring soils and sand pixels that may be showing more reflectance than vegetation (Barati et al 2011). Surrounding soils represent visible wavelengths and will continue to affect traditional vegetation indices that commonly use red wavelengths until soils are fully covered by vegetation (Jackson and Huete 1991). In order to minimize the confusing impacts of soil in the background, soil-adjusted vegetation indices were developed (Carreiras et al 2006). The SAVI was formed (Huete 1988) to minimize soil impacts on canopy spectra by integrating the NDVI denominator into soil adjustment factor (Qi et al 1994). Its results are presented based on cotton canopies measured by ground and aircraft. It has been observed that the MSAVI increases the vegetation signal's dynamic range while reducing soil background impacts, that leads to increased vegetation sensitivity as explained by a soil noise ratio of “vegetation signal” (Kasawani et al 2010). In sparsely vegetated areas, such as mangrove swamps (Kasawani et al 2010) and deserts (Barati et al 2011), SAVI has been found to work more effectively than NDVI. Taking into account the vegetation condition in Haryana, which is characterized by fairly open canopies, the soil-adapted indices have been evaluated in the present study.

The complexity of the ecological environment, however, makes the limits of typical environmental surveys and statistics apparent. The study methodologies and depth were enhanced with the use of new technologies, including RS and GIS (Geographic information system) in the eco-environmental evaluation (Zhang et al 2011). However, a few studies compared the variations and applications of these indices for the state of Haryana. The state of Haryana was chosen as the case study region for the investigation and quantitative evaluation of this work. Eco-environmental indices from 2013 to 2018 were examined and evaluated with the help of GIS and RS technology, which could be helpful for governments in formulating policies to protect the environment. The primary objective of this research was to identify the hot spots of water stress, vegetation vulnerability, and temperature variation for sustainable development with environment protection.

MATERIAL AND METHODS

Study area: The study area included seven stations located in seven different districts (Ambala Bhiwani, Gurugram, Hisar, Karnal, Narnaul, and Rohtak) of Haryana state (Fig. 1).

The site is situated between the latitudes of 27°39'20" to 30°55'05" N and longitudes of 74°27'08" to 77°36'05" E. The total geographical area of the state is 44,212 km2 and is located in the NW of India. The study region is subjected to arid to semi-arid monsoon climatic conditions with an average annual rainfall of 450 mm. In summer, the state experiences extremely hot temperatures of about 45°C (Singh 2010), whereas in winter, it becomes mild. During the Monsoon (June-Sept), approximately 80% of the rainfall is received, while the Remaining 20 % is received in winter season (Singh 2010) due to western disturbance.

Data used: The data used in this study are seven scenes of OLI (Operational Land Imager), Landsat-8 (Path 146/Row

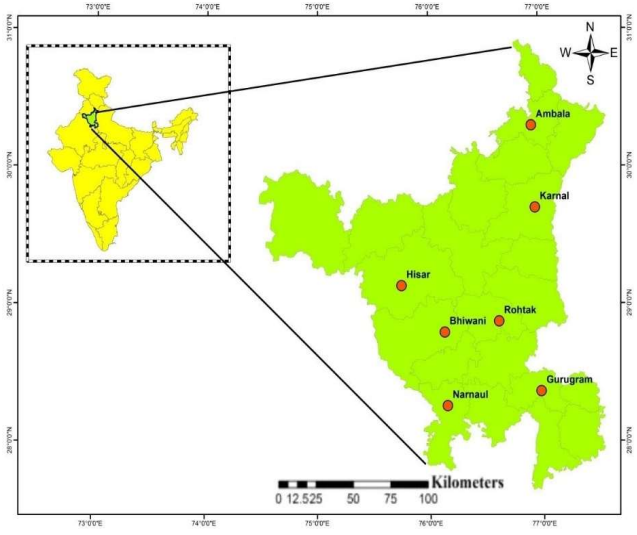

Fig. 1. Study area

40, Path 146/Row 41, Path 147/Row 39, Path 147/Row 40, Path 147/Row 41, Path 148/Row 39, and Path 148/Row 40) obtained from Earth Explorer (http://earthexplorer.usgs.gov/, accessed on 1 February 2019) with different acquisition dates ranging from 2013 to 2018, and which are cloud-free images. The Landsat-8 sensor provides 30 m spatial resolution data with 11 spectral bands.

Software used: ArcGIS was used for database creation, spatial analysis, and map preparation. ERDAS (Earth Resources Data Analysis System) Imagine was used for image processing and determination of vegetation and water indices (Islam et al 2018).

Methodology: Satellite-based images for Landsat-8 were processed for the estimation of nine indicators, namely Surface Albedo, NDVI, SAVI, MSAVI, NDBI, NDWI, NDMI, NDIIB7, and LST. These indicators were assessed for the Monitoring of vegetation health, water stress, and temperature variation, having 30 m spatial resolution for 2013 to 2018.

Vegetation/water indices: Landsat-8 OLI surface reflectance was used to calculate surface albedo and vegetation indices. Bands 1-7 surface reflectance was used to calculate vegetation indices and albedo. For generating LST, the brightness temperature of band 10 was used (Table 1).

Surface albedo estimation: The albedo (α) was calculated according (Smith 2010)'s to algorithm. The broadband surface albedo was calculated as band integration with a specified value, as shown in Equation 1:

$$\alpha = \frac{0.356B_2 + 0.130B_4 + 0.373B_5 + 0.085B_6 + 0.072B_7 - 0.0018}{0.356 + 0.130 + 0.373 + 0.085 + 0.072} \quad (1)$$

where B_2, B_4, B_5, B_6, and B_7 represent blue, red, near-infrared, middle-infrared, and far-infrared bands of multispectral Landsat-8, respectively.

Land surface temperature estimation (LST): Brightness temperature was estimated using TIR (Thermal Infrared) band 10, and NDVI was calculated using bands 4 and 5 in the optical range from the Landsat satellite images. The algorithm was executed in ERDAS Imagine, taking inputs from the metadata file available with the downloaded images. The steps involved in LST calculation are as follows:

Top of atmosphere radiance calculation: The TIR band 10 values were converted into the top of atmosphere (TOA) spectral radiance (Lλ) using the formula obtained from(Li and Jiang 2018) and given in Equation 2:

$$L\lambda = M_L * Q_{cal} * A_L - O_i \quad (2)$$

where M_L is the band-specific multiplicative rescaling factor, Q_{cal} is the Band 10 image, A_L is the band-specific rescaling factor, and O_i is the band 10 correction (Barsi et al 2014).

Radiance to at-sensor temperature conversion: Using the thermal constants from the metadata file, the TIR band 10DN (Digital Number) values were transformed from spectral radiance to brightness temperature (BT) using Equation 3 (Li and Jiang 2018):

$$BT = \frac{K_2}{\ln[(K_1/L\lambda) + 1]} - 273.15 \quad (3)$$

where K_1 and K_2 stand for the band-specific thermal conversion constants from the metadata (K_1 and K_2 constant for Band x, where x is the thermal band number). For obtaining the results in degrees Celsius, the radiant temperature was calculated by adding absolute zero (approx. −273.15°C) (Xu and Chen 2004).

Calculation of vegetation proportion (P_v): The vegetation proportion (P_v) was calculated according to (Wang et al 2015, Kumar et al 2021b) using Equation 4:

$$P_v = \left(\frac{NDVI - NDVI_{min}}{NDVI_{max} - NDVI_{min}}\right)^2 \quad (4)$$

The NDVI values are different for each region, whereas $NDVI_{max}$ and $NDVI_{min}$ depend on the vegetation condition (Jimenez-Munoz et al 2009).

Land surface emissivity: The emissivity of the land surface (ε) must be known to estimate LST. LSE is a proportionality factor that scales black body radiance (Planck's law) to predict emitted radiance. It is the efficiency of transmitting thermal energy throughout the surface into the atmosphere (Jimenez-Munoz et al 2006). The determination of the ground emissivity is calculated using Equation 5 (Sobrino et al 2004).

$$\varepsilon_\lambda = \varepsilon_{v\lambda} \times P_V + \varepsilon_{s\lambda}(1 - P_v) + C_\lambda \quad (5)$$

where the vegetation and soil emissivity are ε_v and ε_s, respectively. C reflects the roughness of the surface (C = 0 for homogenous and flat surfaces). It was taken as a constant value of 0.005 (Sobrino and Raissouni 2000).

LST retrieval: The LST retrieval or the land surface temperature (Ts) corrected by emissivity was computed using Equation 6:

$$T_s = \frac{BT}{[1 + \{(\lambda BT/\rho) \ln \varepsilon_\lambda\}]} \quad (6)$$

where T_s is the LST in Celsius (°C), BT is Brightness Temperature (°C) at the sensor, and λ is the wavelength of radiance emitted. The maximum response and the limiting wavelength average (λ = 10.895) were used (Markham and Barker 1985).

RESULTS AND DISCUSSION

Normalized difference vegetation index (NDVI): There are wide variations in NDVI at different locations, which may be considered substantial for representing all the vegetation existing in the state (Fig. 2). The lowest NDVI value was observed for Rohtak station (0.08) in May 2015, while the maximum for Gurugram (0.35) in December 2017. The values of NDVI at different locations are used for analyzing the spatial distribution of changes in NDVI values during the Rabi and *Kharif* seasons. Similar trends in NDVI (-0.2 to 0.52) were also shown by earlier scientist (Bala et al 2015, Swain and Barik 2015, Tyagi et al 2019). NDVI variations may be due to the fallow land between the period of *Rabi* and *Kharif* crops, which is also responsible for the increase in temperature. Moreover, once the SW monsoon sets in, it leads to an increase in vegetation cover in the study area, thereby increasing NDVI values during that period Mathew et al 2016).

Soil-adjusted vegetation index (SAVI): The maximum of SAVI was observed for Karnal and Gurugram stations during September and October 2017, respectively, whereas the lowest value was obtained for Rohtak station in May 2016 (Fig. 3). The variation in SAVI may be due to higher temperatures during May month. Further, the lower rainfall

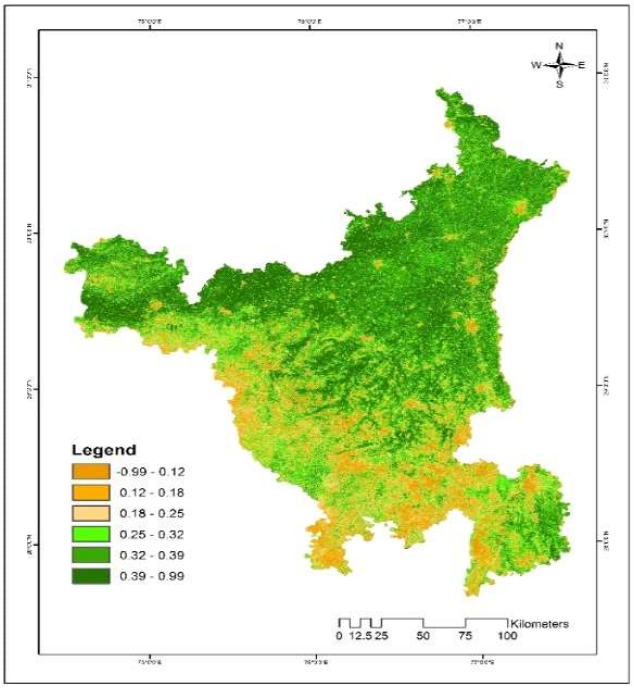

Fig. 2. Spatial variation of NDVI over the study region

Table 1. Vegetation indices evaluation formula for Landsat 8

	Acronym	Equation	Source
Vegetation Greenness Indices	SAVI	$1.5 \times \frac{B5 - B4}{B5 + B4 + 0.5}$	(Huete 1988)
	MSAVI	$\frac{2 \times B5 + 1 - \sqrt{2 \times B5 + 1\ ^2 - 8 \times\ B5 - B4}}{2}$	(Qi et al 1994)
	NDVI	$\frac{B5 - B4}{B5 + B4}$	(Tucker 1979)
Vegetation Water Indices	NDMI	$\frac{B5 - B6}{B5 + B6}$	(Wilson and Sader 2002)
	NDWI	$\frac{B3 - B5}{B3 + B5}$	(McFeeters 1996)
	NDIIB7	$\frac{B5 - B7}{B5 + B7}$	(Hunt and Rock 1989)
	NDBI	$\frac{B6 - B5}{B6 + B5}$	(Zha et al 2003)

Note: B represents band and numbering indicates band number

during the season led to large variations in SAVI values during these months (Swain and Barik 2015, Tyagi et al 2019).

Modified soil-adjusted vegetation index (MSAVI): The MSAVI varied from -0.38 to 0.74. The highest MSAVI was observed in the northern part of the study area while the southern part shows the lowest indices (Fig. 4). The lowest MSAVI was observed at Hisar station in June 2016 which falls under a semi-arid region and was highest for Gurugram station in September 2017. The MSAVI values were affected by the type and density of vegetation, soil texture, and the prevailing climatic conditions during the season. Tyagi et al (2019) reported a slightly higher value of MSAVI, mainly due to the difference in location and the climatic conditions.

Normalized difference moisture index (NDMI): The NDMI showed wide variations in the study area which varied from -0.99 to 0.99 (Fig. 5). The maximum value of NDMI was observed in October 2017 at Karnal station, whereas was lowest in May 2013 for Hisar station. The NDMI values varied largely due to changes in temperature, water availability (low), and vegetation conditions during the growing season (Das et al 2017). The land cover was very low in May due to the absence of any crops. Moreover, the rainfall usually arrives during the monsoon season (first week of June). Thus, there was no additional source of moisture/irrigation during the month, leading to lower values of NDMI.

Normalized difference water index (NDWI): NDWI spatial

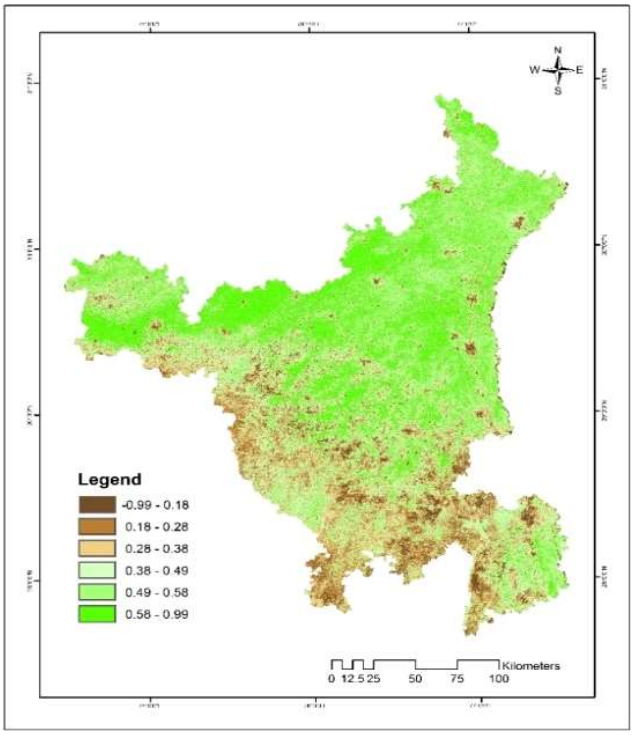

Fig. 3. Map of SAVI

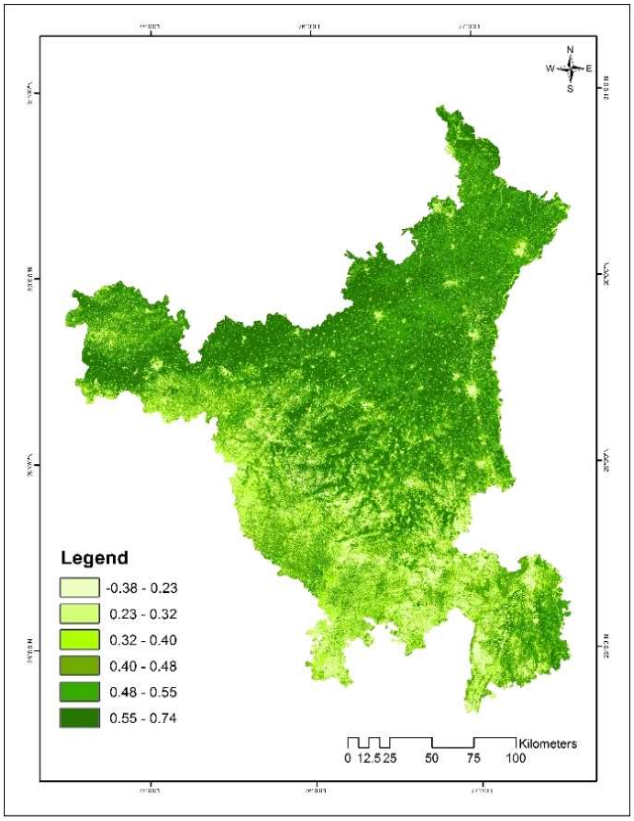

Fig. 4. Map of MSAVI

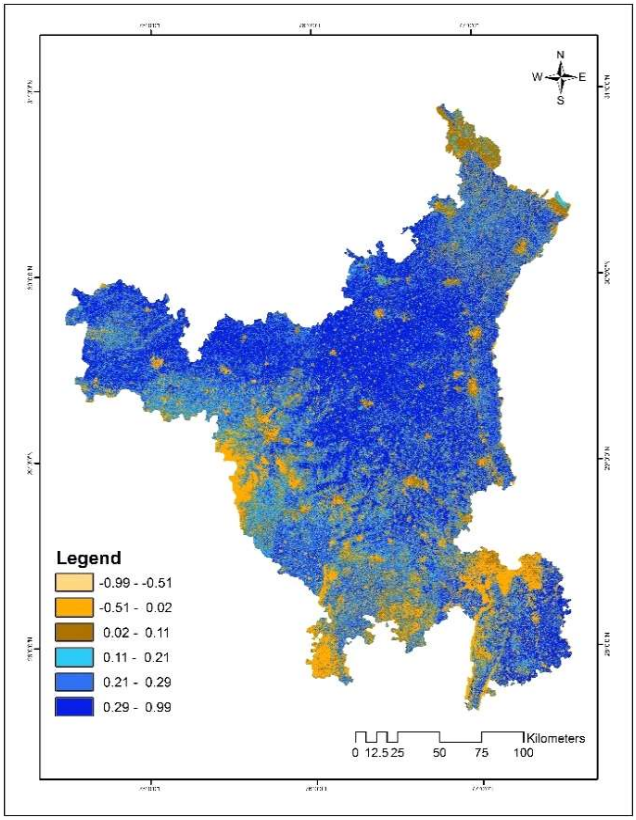

Fig. 5. Map of NDMI

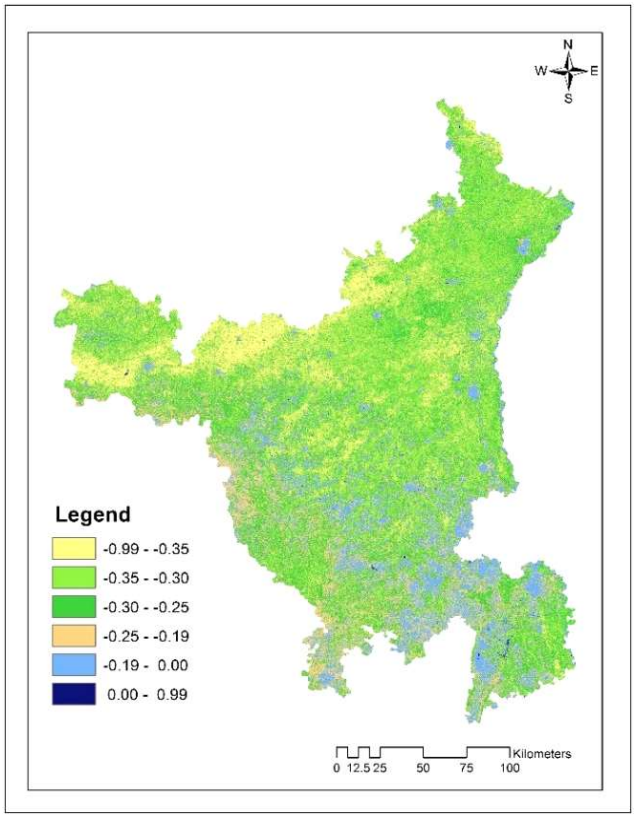

Fig. 6. Map of NDWI

variation in the study area which ranges from -0.99 to 0.99 (Fig. 6). The results indicated the lowest value of NDWI at Gurugram station in September 2017, while the highest value was at Hisar station in November 2013. The maximum study area showed negative NDWI which indicate the water scarcity during the study period. Similar observation on NDWI was observed by Bala et al 2015.

Normalized difference infrared index for band 7 (NDIIB7): NDIIB7 varied from -0.99 to 0.99 (Fig. 7). The highest and lowest was observed at Karnal station in October 2017 and Hisar station in May 2013, respectively. The variation in NDIIB7 values indicated that the vegetation was under water stress.

Normalized difference built-up index (NDBI): The spatial variation shows the small variation throughout the study area (Fig. 8). Almost all over the Haryana state, the NDBI ranged from -99 to -0.13 and negative values indicate the absence of buildings or other permanent structures in the study area (Sharma and Joshi 2015, Jangra and Kaushik 2017). The values of NDBI ranged between −0.17 and 0.00. Among the seven districts of the state, the maximum NDBI value of 0.00 was recorded for Rohtak district in December 2014, while the minimum (−0.17) was for Karnal in October 2017.

Surface albedo: The surface albedo was highest at Ambala station in September 2015, while the lowest value was at

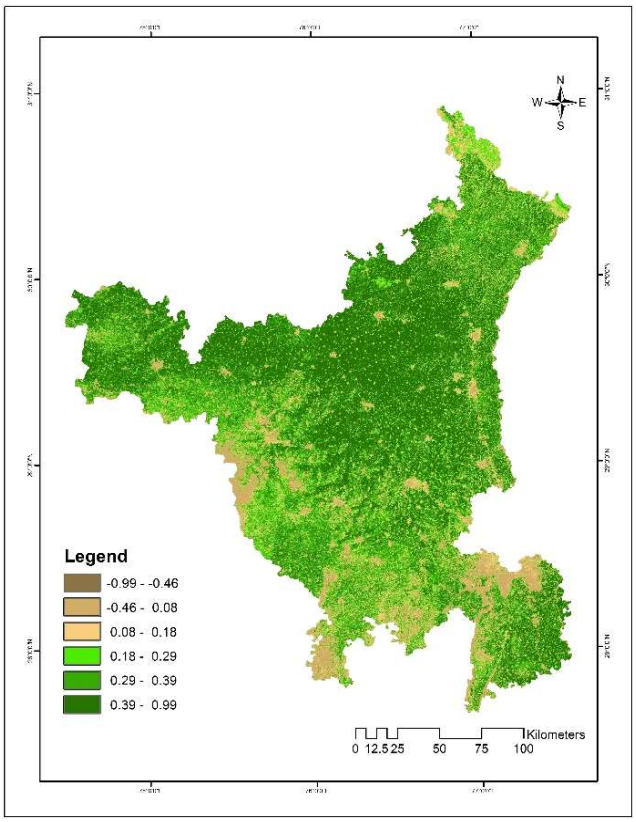

Fig. 7. Map of NDIIB7

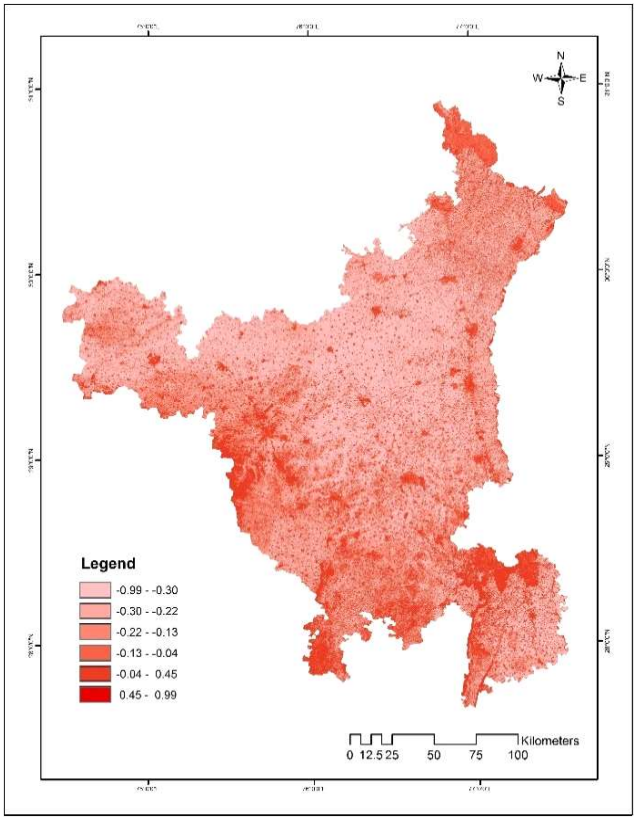

Fig. 8. Map of NDBI

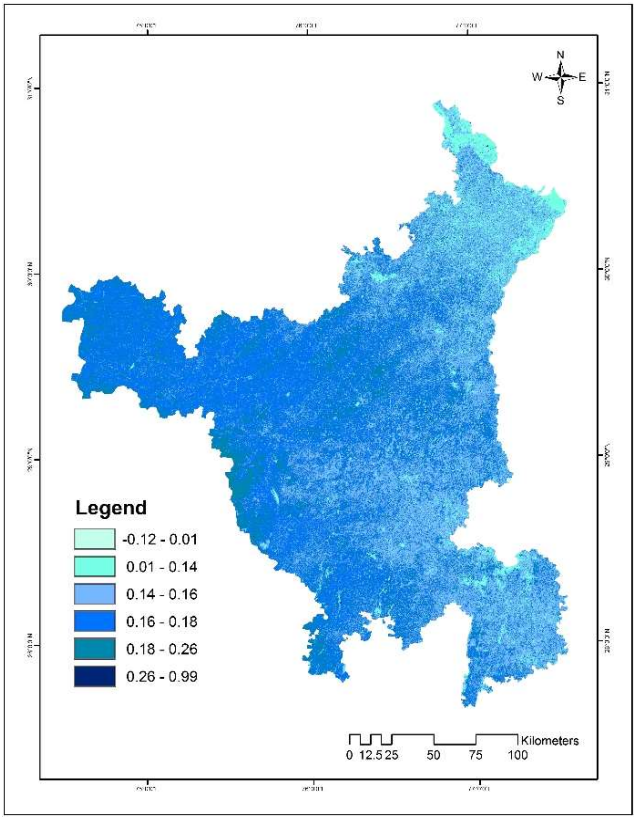

Fig. 9. Map of surface Albedo

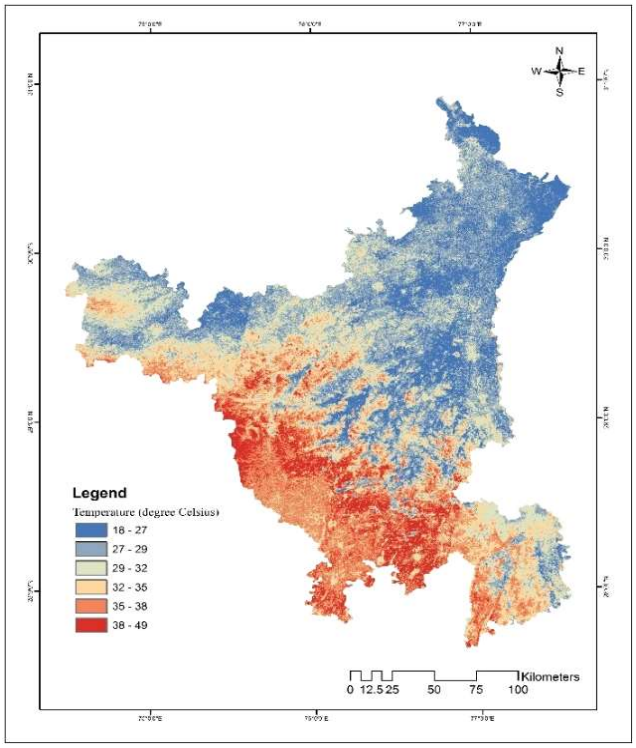

Fig. 10. Map of LST

Narnaul station in 2017 December (Fig. 9). The albedo values showed little variation due to similar climatic and geographic conditions over the whole study area. Mathew et al (2016) showed a small variation in the surface albedo values as compared to the present study.

Land surface temperature (LST) : LST varied from 18 to 49^{0}C throughout the study area (Fig. 10). The northern part of the study area shows the lowest LST while the southern part shows the highest LST. The maximum LST value was observed in May and the lowest was in December. The probable reason for this is that the heat waves flow prominently in the region during May and June which leads to an increase in LST, while cold waves are dominant in December and January when lowest the temperature was during these months.

CONCLUSIONS

There is a wide range of variation in vegetation and water indices throughout the year at different locations during the study period. This variation is mainly due to the flow of heat waves in the region during May and June, leading to an increase in temperature, while cold waves are dominant during December. The computed indices proved to be useful for assessing stress levels in different types of vegetation in the study area. The results indicated a sudden increase in LST and fall in vegetation and water indices values during May and June, as the land remained fallow intermittently after the harvesting of crops, thus leading to an increase in temperature. During the monsoon, an increase in vegetation cover and water was recorded, which in turn indicated increased vegetation and water indices. Moreover, it was observed that the indices were affected by the type and density of vegetation, soil texture, and the prevailing climatic conditions during different seasons. The variations in the values of different indices can be attributed to the varied range of temperatures, water availability, and vegetation condition during different cropping seasons. It is concluded that these indices would provide great help to monitor vegetation health, water stress, and temperature variations in the study area. Thus, the remote-sensing-based monitoring and assessment of vegetation health, water stress, and temperature variation would be helpful in long-term crop planning in a region. Such a study is not limited simply to monitoring and assessing the vegetation health, water stress, and temperature variation in a region. There exists a scope to integrate the data generated from different indices for estimating the performance of the crops grown in the region concerning the available input information.

REFERENCES

Arvind, Hooda RS, Sheoran HS, Kumar D, Satyawan, Abhilash and Bhardwaj S 2020. RS-based regional crop identification and

mapping : A case study of Barwala sub- branch of Western Yamuna Canal in Haryana (India). *Indian Journal of Traditional Knowledge* **19**(1): 182-186.

Bala A, Rawat KS, Misra A and Srivastava A 2015. Vegetation indices mapping for Bhiwani district of Haryana (India) through LANDSAT-7ETM+ and remote sensing techniques. *Journal of Applied and Natural Science* **7**(2): 874-879.

Barati M, Esfahani S and Utigard TA 2011. Energy recovery from high temperature slags. *Energy* **36**(9): 5440-5449.

Barsi JA, Schott JR, Hook SJ, Raqueno NG, Markham BL and Radocinski RG. 2014. Landsat-8 thermal infrared sensor (TIRS) vicarious radiometric calibration. *Remote Sensing* **6**(11): 11607-11626.

Bausch W, Trout T and Buchleiter G 2011. Evapotranspiration adjustments for deficit-irrigated corn using canopy temperature: A concept. *Irrigation and Drainage* **60**(5): 682-693.

Boori MS, Choudhary K, Paringer R and Kupriyanov A 2022. Using RS/GIS for spatiotemporal ecological vulnerability analysis based on DPSIR framework in the Republic of Tatarstan, Russia. *Ecological Informatics* **67**(1): 101490.

Carreiras JM, Pereira JM and Pereira JS and Carreiras J 2006. Estimation of tree canopy cover in evergreen oak woodlands using remote sensing. *Forest Ecology and Management* **223**(1-3): 45-53.

Chaitanya TP, Singh UK and Agarwal S 2021. Forest fire monitoring of wildlife sanctuary using geospatial techniques. *Indian Journal of Ecology* **48**(3): 681-685.

Das PK, Sahay B, Seshasai MV and Dutta D 2017. Generation of improved surface moisture information using angle-based drought index derived from Resourcesat-2 AWiFS for Haryana state, India. Geomatics, *Natural Hazards and Risk* **8**(2): 271-281.

DeJonge KC, Mefford BS and Chavez JL 2016. Assessing corn water stress using spectral reflectance. *International Journal of Remote Sensing* **37**(10): 2294-2312.

DeJonge KC, Taghvaeian S, Trout TJ and Comas LH 2015. Comparison of canopy temperature-based water stress indices for maize. *Agricultural Water Management* **156**: 51-62.

Dwivedi RS and Sreenivas K 2002. The vegetation and waterlogging dynamics as derived from spaceborne multispectral and multitemporal data. *International Journal of Remote Sening* **23**(14): 2729-2740.

Gu Y and Wylie BK 2015. Downscaling 250-m MODIS growing season NDVI based on multiple-date Landsat images and data mining approaches. *Remote Sensing* **7**(4): 3489-3506.

Huete AR 1988. A soil-adjusted vegetation index (SAVI). *Remote Sensing of Environment* **25**(3): 295-309.

Hunt Jr ER and Rock BN 1989. Detection of changes in leaf water content using Near-and Middle-Infrared reflectances. *Remote Sensing of Environment* **30**(1): 43-54.

Islam K, Jashimuddin M, Nath B and Nath TK 2018. Land use classification and change detection by using multi-temporal remotely sensed imagery: The case of Chunati wildlife sanctuary, Bangladesh. *The Egyptian Journal of Remote Sensing and Space Science* **21**(1): 37-47.

Jackson, RD and Huete AR 1991. Interpreting vegetation indices. *Preventive Veterinary Medicinev* **11**(3-4): 185-200.

Jangra, R and Kaushik SP 2017. A spatial analysis of residential land values in Kaithal City, Haryana, India. *International Journal of Advancement in Remote Sensing, GIS and Geography* **3**(2): 1-15.

Jimenez-Munoz JC, Sobrino JA, Gillespie A, Sabol D and Gustafson WT 2006. Improved land surface emissivities over agricultural areas using ASTER NDVI. *Remote Sensing of Environment* **103**(4): 474-487.

Jimenez-Munoz JC, Sobrino JA, Plaza A, Guanter L, Moreno J and Martínez P 2009. Comparison between fractional vegetation cover retrievals from vegetation indices and spectral mixture analysis: Case study of PROBA/CHRIS data over an agricultural area. *Sensors* **9**(2): 768-793.

Johnson LF and Trout TJ 2012. Satellite NDVI assisted monitoring of vegetable crop evapotranspiration in California's San Joaquin Valley. *Remote Sensing* **4**(2): 439-455.

Kasawani I, Norsaliza U and Mohdhasmadi I 2010. Analysis of spectral vegetation indices related to soil-line for mapping mangrove forests using satellite imagery. *Applied Remote Sensing Journal* **1**: 25-31.

Kumar, D, Arvind, Nain AS, Darshana, Arya S, Bhardwaj S and Abhilash 2019. Soil loss estimation using geo-spatial technology in north western trai region of India. *Journal of Agrometeorology* **21**: 182-188.

Kumar D, Arvind, Nain AS, Singh A, Mor A and Bhardwaj S 2021a. Geo-spatial technology application for prioritization of land resources in Udham Singh Nagar District of Uttarakhand, India. *Indian Journal of Traditional Knowledge* **20**(2): 595-603.

Kumar D, Dhaloiya A, Nain AS, Sharma MP and Singh A. 2021b. Prioritization of watershed using remote sensing and geographic information system. *Sustainability* **13**(16): 9456.

Li S and Jiang GM 2018. Land Surface Temperature Retrieval From Landsat-8 Data with the Generalized Split-Window Algorithm. *IEEE Access* **6**: 18149-18162.

Markham BL and Barker JL 1985. Spectral characterization of the LANDSAT Thematic Mapper sensors. *International Journal of Remote Sensing* **6**(5): 697-716.

Mathew A, Khandelwal S and Kaul N 2016. Spatial and temporal variations of urban heat island effect and the effect of percentage impervious surface area and elevation on land surface temperature: Study of Chandigarh city, India. *Sustainable Cities and Society* **26**: 264-277.

McFeeters SK 1996. The use of the Normalized Difference Water Index (NDWI) in the delineation of open water features. *International Journal of Remote Sensing* **17**(7): 1425-1432.

Mikkili S and Agarwal SKPS 2021. Gis-based integrated approach for sustainable management of ecology and environment with green and blue spaces. *Indian Journal of Ecology* **48**(3): 931-938.

Qi J, Chehbouni A, Huete AR, Kerr YH and Sorooshian SA 1994. A modified soil adjusted vegetation index. *Remote Sensing of Environment* **48**(2): 119-126.

Saha S, Sarkar R, Roy J, Hembram TK, Acharya S, Thapa G and Drukpa D 2021. Measuring landslide vulnerability status of Chukha, Bhutan using deep learning algorithms. *Scientific Reports* **11**(1):16374.

Sharma R and Joshi PK 2015. The changing urban landscape and its impact on local environment in an Indian megacity: The case of Delhi. *Urban Development Challenges, Risks and Resilience in Asian Mega Cities*. Springer: 61-81.

Singh D 2010. Contingency Crop Plan for Pearl Millet in Western Agroclimatic Zone of Haryana. AICRP on Agrometeorology, Department of Agricultural Meteorology, CCS Haryana Agricultural University.

Smith RB 2010. The heat budget of the earth's surface deduced from space. Page Y*ale University Center for Earth Observation: New Haven,* CT, USA.

Sobrino JA, Jimenez-Munoz JC and Paolini L 2004. Land surface temperature retrieval from LANDSAT TM 5. *Remote Sensing of Environment* **90**(4): 434-440.

Sobrino JA and Raissouni N 2000. Toward remote sensing methods for land cover dynamic monitoring: Application to Morocco. *International Journal of Remote Sensing* **21**(2): 353-366.

Surya B, Ahmad DN, Sakti HH and Sahban H 2020. Land use change, spatial interaction, and sustainable development in the metropolitan urban areas, South Sulawesi Province, Indonesia. *Land* **9**(3): 95.

Swain AK and Barik KK 2015. Spatial greening pattern estimation of Himachal Pradesh, India using IRS-P6 AWiFS seasonal data. *International Journal of Science and Research* **4**: 1501-1505.

Taloor AK, Manhas DS and Kothyari GC 2021. Retrieval of land surface temperature, normalized difference moisture index, normalized difference water index of the Ravi basin using Landsat data. *Applied Computing and Geosciences* **9**:100051.

Trout TJ, Johnson LF and Gartung J 2008. Remote sensing of canopy cover in horticultural crops. *HortScience* **43**(2): 333-337.

Tucker CJ 1979. Red and photographic infrared linear combinations for monitoring vegetation. *Remote Sensing of Environment* **8**(2): 127-150.

Tyagi J, Kumar C and Somvanshi S 2019. Remote sensing approach to identify salt affected soil in agricultural land of Gautam Buddha Nagar District. *Journal of Agroecology and Natural Resource Management* **6**: 84-87.

Wang F, Qin Z, Song C, Tu L, Karnieli A and Zhao S 2015. An improved mono-window Algorithm for land surface temperature retrieval from Landsat 8 thermal infrared sensor data. *Remote Sensing* **7**(4): 4268-4289.

Wilson EH and Sader SA 2002. Detection of forest harvest type using multiple dates of Landsat TM imagery. *Remote Sensing of Environment* **80**(3): 385-396.

Xu H 2006. Modification of normalised difference water index (NDWI) to enhance open water features in remotely sensed imagery. *International Journal of Remote Sensing* **27**(14): 3025-3033.

Xu HQ and Chen BQ 2004. Remote sensing of the urban heat island and its changes in Xiamen City of SE China. *Journal of Environmental Sciences* **16**(2): 276-281.

Xu J, Renaud FG and Barrett B 2021. Modelling land system evolution and dynamics of terrestrial carbon stocks in the Luanhe River Basin, China: A scenario analysis of trade-offs and synergies between sustainable development goals. *Sustainability Science* :1-23.

Zha Y, Gao J and Ni S 2003. Use of normalized difference built-up index in automatically mapping urban areas from TM imagery. *International Journal of Remote Sensing* **24**(3): 583-594.

Zhang Z, Ming D and Xing T 2011. Eco-environmental monitoring and evaluation of the Tekes Watershed in xinjiang using remote sensing images. *Procedia Environmental Sciences* **10**: 427-432.

Received 25 March, 2023; Accepted 01 June, 2023